JOURNAL OF BACTERIOLOGY, Nov. 1993, p. 6945–6952
0021-9193/93/216945-08$02.00/0

Vol. 175, No. 21

Physical Map of the Genome of *Rhizobium meliloti* 1021

RHONDA J. HONEYCUTT,* MICHAEL McCLELLAND, AND BRUNO W. S. SOBRAL

California Institute of Biological Research, 11099 North Torrey Pines Road, Suite 300, La Jolla, California 92037

Received 7 June 1993/Accepted 3 September 1993

A physical map of the genome of *Rhizobium meliloti* 1021 is presented. The physical sizes of the three replicons in this genome had previously been determined and are as follows: the chromosome, 3.4 Mb; pSym-b, 1.7 Mb; and pSym-a, 1.4 Mb. The physical maps for this GC-rich genome contain AT-rich restriction sites for *Swa*I (5′-TAAATTTA-3′), *Pac*I (5′-TTAATTAA-3′), *Pme*I (5′-GTTTAAAC-3′), and, for pSym-b, *Spe*I (5′-ACTAGT-3′). In addition, the endonuclease I-*Ceu*I cleaved the 23S rRNA genes in this genome, and perhaps in most eubacterial genomes. I-*Ceu*I digestion and polymerase chain reaction amplification of *rrn* regions were used to determine that there are at least three *rrn* loci in *R. meliloti*, all of which are located on the chromosome. The orientation of the *rrn* loci was determined by Southern blotting with probes from *rrn* sequences located 5′ and 3′ to the I-*Ceu*I site. The *rrn* loci are clustered in one part of the chromosome and are oriented so that transcription will occur away from a single point in the circle, as observed for the origin of replication in the *Escherichia coli* and *Salmonella typhimurium* chromosomes. Fifteen genes that had been tagged by Tn*5* insertion were localized to fragments on the chromosome physical map by using the IS*50* as a probe in Southern blots. In addition, *glt* and *gap* were placed on the physical map by using Southern hybridization with cloned genes. The fortuitous occurrence of a *Spe*I site in Tn*5-233* was used to physically map 10 genetically mapped Tn*5-233* integrations on pSym-b and to anchor the physical map to the genetic map. Finally, we demonstrate the usefulness of the map by localizing a total of 12 previously unmapped transposon insertions in the genome. This is the first physical map of the genome of a multireplicon member of the family *Rhizobiaceae* as well as the first physical map of a *Rhizobium* chromosome.

Restriction maps have been constructed for over a dozen bacterial species with endonucleases that cleave infrequently (26) and then by separation of the resulting fragments by pulsed-field gel electrophoresis (PFGE) (34). Physical maps are particularly useful for poorly studied organisms in which genetic manipulations are tedious or difficult, as is the case with many agriculturally important gram-negative bacteria. Because of the strict correlation of physical and genetic maps in bacteria (18), physical maps aid in mapping new markers or mutations, in directing gene-cloning and fine-mapping efforts, and in evolutionary studies (19, 32).

Physical maps for the entire genome of only two of the agronomically important members of the family *Rhizobiaceae* have been undertaken: *Bradyrhizobium japonicum* (20) and *Rhizobium meliloti* (35, 36). These two genera of symbiotic, nitrogen-fixing bacteria differ markedly in their genomic architectures (25) and evolutionary histories (14). The *B. japonicum* genome consists of a single large chromosome (8.7 Mb), with symbiotic functions clustered in a 400-kb region (20), and this organism is phylogenetically distinguished from *R. meliloti* on the bases of 16S rRNA analysis (14) and biochemical functions (17). In contrast, the *R. meliloti* genome is more complex in structure, with symbiotic and catabolic genes scattered among at least three replicons (two so-called megaplasmids [pSym-a and pSym-b] and the chromosome [3, 16]), and it is more closely related to *Agrobacterium tumefaciens* than to *B. japonicum* (14). Furthermore, in *R. meliloti*, many of the genes involved in nodule formation and nitrogen fixation (25, 36) are found on megaplasmids (8, 16).

Circular genetic maps of the chromosome (4, 13, 27) and of pSym-b (5) of *R. meliloti* 1021 have been constructed. No complete, circular genetic map exists for pSym-a. The physical map of a 500-kb symbiotic plasmid from *Rhizobium* sp. strain NGR234 has been established (28). Although small regions containing cloned genes have been mapped with restriction enzymes, no circular physical maps exist for any of the replicons of *R. meliloti*, the best characterized of the *Rhizobiaceae*. We set out to physically map the entire genome of *R. meliloti* 1021 and herein report the results.

MATERIALS AND METHODS

Strains, plasmids, and growth conditions. The bacterial strains and plasmids used in this study are listed in Table 1. Cultures of *R. meliloti* were grown in L broth (33) supplemented with 2.5 mM $CaCl_2$ and the appropriate antibiotic (200 μg of streptomycin [Str], 100 μg of neomycin [Nm], 0.5 μg of oxytetracycline [Ot], 10 μg of gentamicin [Gm], 50 μg of spectinomycin [Sp], or 10 μg of rifampin [Rif] ml^{-1}).

PFGE and Southern hybridization procedures. Genomic DNAs were prepared in agarose plugs and digested with restriction endonucleases as reported by Sobral et al. (35). Unless otherwise noted, all chemicals were purchased from Sigma Chemical Co. (St. Louis, Mo.), and restriction enzymes were purchased from New England Biolabs (Boston, Mass.), Boehringer Mannheim (Indianapolis, Ind.), or Stratagene (La Jolla, Calif.). PFGE of total genomic DNA and separated replicons in transverse alternating electric fields (TAFE) was done as reported by Sobral et al. (36). DNA fragments used as probes were radiolabelled with [α-^{32}P]dCTP using a Prime-It II kit (Stratagene), and Southern hybridizations were done under standard high-stringency conditions (33). For hybridizations to Tn*5*-containing strains, the IS*50* element was isolated as a 1.0-kb *Pst*I fragment from pGS220 (Table 1). The sizes of restriction enzyme fragments and hybridization signals were determined as described by Sobral et al. (36).

* Corresponding author. Electronic mail address: sobralab@lifsci.sdsu.edu.

TABLE 1. Bacterial strains and plasmids used for mapping

Strain or plasmid	Description	Source[a]
R. meliloti		
1021	Str^r, derivative of 2011	S. Long
5050	*met1023*::Tn*5*	G. Walker
7558	*lpsB*::Tn*5-104-3*	G. Walker
8611	Tn*5*-MobΩ612	G. Walker
8612	Tn*5*-MobΩ614	G. Walker
A1681	*ntrA*::Tn*5*	G. Walker
5418	*gap1*::Tn*5*	T. Finan
5404	Gm^r Sp^r, Ω5040::Tn*5-233* [53°][b]	T. Finan
F675	Ot^r, Ω5188::Tn*5-132* [74°]	T. Finan
F601	Nm^r, Ω5177::Tn*5* [78°]	T. Finan
F560	Gm^r Sp^r, Ω5149::Tn*5-233* [82°]	T. Finan
F570	Nm^r, Ω5159::Tn*5* [167°]	T. Finan
F532	Gm^r Sp^r, Ω5143::Tn*5-233* [189°]	T. Finan
F470	Nm^r, Ω5133::Tn*5* [226°]	T. Finan
F221	Nm^r, Ω5061::Tn*5-235* [241°]	T. Finan
F303	Gm^r Sp^r, Ω5098::Tn*5-233* [264°]	T. Finan
5435	Gm^r Sp^r, Ω5047::Tn*5-233* [282°]	T. Finan
F220	Gm^r Sp^r, Ω5060::Tn*5-233* [289°]	T. Finan
GMI395	Sm^r Nm^r Rif^r, *fixL*::Tn*5*	J. Batut
GM1708ΔJB16	Nm^r Rif^r, mu*dII1734*	J. Batut
N3	Tn*5luxAB*, luciferase induction by N$^-$ starvation	F. de Bruijn
N4	Tn*5luxAB*, luciferase induction by N$^-$ starvation	F. de Bruijn
N5	Tn*5luxAB*, luciferase induction by N$^-$ starvation	F. de Bruijn
N12	Tn*5luxAB*, luciferase induction by N$^-$ starvation	F. de Bruijn
N25	Tn*5luxAB*, luciferase induction by N$^-$ starvation	F. de Bruijn
N110	Tn*5luxAB*, luciferase induction by N$^-$ starvation	F. de Bruijn
N112	Tn*5luxAB*, luciferase induction by N$^-$ starvation	F. de Bruijn
N113	Tn*5luxAB*, luciferase induction by N$^-$ starvation	F. de Bruijn
N183	Tn*5luxAB*, luciferase induction by N$^-$ starvation	F. de Bruijn
aux7	Leu$^-$ Fix$^-$	F. de Bruijn
aux12	Leu$^-$ Nod$^-$ Fix$^-$	F. de Bruijn
aux17	His$^-$	F. de Bruijn
aux18	Arg$^-$	F. de Bruijn
aux35	Trp$^-$	F. de Bruijn
aux36	Leu$^-$ Fix$^-$	F. de Bruijn
aux37	Trp$^-$	F. de Bruijn
aux56	Thl$^-$	F. de Bruijn
aux57	Met$^-$	F. de Bruijn
aux8	Cys$^-$	F. de Bruijn
aux11	Met$^-$	F. de Bruijn
aux13	Met$^-$ Fix$^-$	F. de Bruijn
aux21	Trp$^-$	F. de Bruijn
aux26	Met$^-$	F. de Bruijn
aux42	Trp$^-$ Fix$^-$	F. de Bruijn
aux47	Trp$^-$	F. de Bruijn
Plasmids		
pTL001	Tet^r, pLAFR1::25-kb *Eco*RI (*glt*)	J. Botsford
pDOB13	Amp^r, pUC9::2.7-kb *Sal*I (*ndvA*)	G. Ditta
exo61.614	Amp^r, BSKS$^+$::1.6-kb *Hin*dIII-*Cla*I (*exoJGF* [26°])	J. Reed
pBB127	Amp^r, pUC8::6.0-kb *Hin*dIII (*dctABD* [115°]	R. Watson
pTH38	Tet^r, pRK7813::7.3-kb *Bam*HIII (*ndvF* [324°])	T. Finan
pGS220	Amp^r Kan^r, pGS330::Tn*5*	T. Finan
pRmJ1	Amp^r, pBR325::8.7-kb *Eco*RI (*nodDABC*)	S. Long
pCHK12	Amp^r, pUC9::3.7-kb *Eco*RI (*nifHD*)	M. Sadowsky

[a] S. Long, Department of Biological Sciences, Stanford University, Stanford, Calif.; G. Walker, Department of Biology, Massachusetts Institute of Technology, Cambridge; T. Finan, Biology Department, McMaster University, Hamilton, Ontario, Canada; J. Batut, INRA-CNRS, Toulouse, France; F. de Bruijn, Center for Microbial Ecology, Michigan State University, East Lansing; J. Botsford, Department of Biology, New Mexico State University, Las Cruces; G. Ditta, Department of Biology, University of California-San Diego, La Jolla; J. Reed, Department of Biology, Massachusetts Institute of Technology, Cambridge; R. Watson, Agriculture Canada, Ottawa, Ontario, Canada; and M. Sadowsky, Department of Microbiology, University of Minnesota, St. Paul.

[b] The genetic-map positions of markers from pSym-b, given in degrees, are converted from kilobase distances reported by Charles and Finan (5).

Preparation of probes from 16S and 23S rRNA genes. The following primers were manufactured by Genosys (Houston, Tex.): 16S-1507, 5′-CCAGATCTGAGCTCAAGGAGGTGA TCCAGC-3′; 16S-11, 5′-GGCTGCAGTCGACGTTTGATC CTGGCTCAG-3′; 23S2790R, 5′-GGGATAACCGCTGAAA GCATCTAAG-3′; and 5S27L2, 5′-CCGTGTTCGGCATGG GAACAGGTGT-3′.

These primers are directed against highly conserved portions of the rRNA genes (29, 39). Polymerase chain reaction (PCR) was done under the conditions reported by Ralph et al.

TABLE 2. Restriction fragments assigned to the *R. meliloti* 1021 chromosome

Enzyme(s)	Designation	Fragment size (kb)[a]	Identifying probe[b]
*Pac*I	Pac no. 1	3,320 ± 300 (7)	*ndvA*
*Pme*I	Pme no. 1	1,825 ± 35 (6)	*ndvA*, *ntrA*, Ω614, *lpsB*, N25, aux12, aux36, aux44, aux56
	Pme no. 3	1,040 ± 20 (6)	*met1023*, N3, aux18, aux35, aux37, aux42, aux47
	Pme no. 4	690 ± 45 (7)	*glt*, *gap1*, N4, N183, aux17, aux49, aux57, 16S*rrn*, 23S and 5S*rrn*
*Swa*I	Swa no. 1	1,820 ± 120 (7)	Ω614, *lpsB*, *gap1*, 16S*rrn*, 23S and 5S*rrn*
	Swa no. 4	620 ± 40 (10)	*ndvA*, glt, 16S*rrn*, 23S and 5S*rrn*
	Swa no. 5	620 ± 40 (10)	SR (contains *Pac*I site)
	Swa no. 6	490 ± 40 (9)	Ω612, *ntrA*, N25, 16S*rrn*, 23S and 5S*rrn*
*Ceu*I	Ceu no. 1	2,700	*lpsB*, Ω614, *ntrA*
	Ceu no. 2	520 ± 20 (11)	*ndvA*, 16S*rrn*
	Ceu no. 3	390 ± 15 (11)	*gap1*, *glt*, 16S*rrn*, 23S and 5S*rrn*
*Pac*I + *Pme*I		895	*ntrA*
		1,020	*lpsB*
*Pac*I + *Swa*I		215	
		360	
*Pac*I + *Ceu*I		2,100	
		615	*ntrA*
*Pme*I + *Swa*I		100	*ndvA*, aux36
		170	*gap1*
		495	*glt*, N4
		585	*lpsB*, Ω614
*Pme*I + *Ceu*I		20	23S and 5S*rrn*
		245	*ndvA*, 16S*rrn*
		260	16S*rrn*
		390	*gap1*, *glt*, 16S*rrn*, 23S and 5S*rrn*
*Swa*I + *Ceu*I		120	16S*rrn*
		170	*gap1*, aux49, 16S*rrn*
		235	*glt*, N4, 23S and 5S*rrn*
		420	*ntrA*, N25, 23S and 5S*rrn*
		400	*ndvA*, 16S*rrn*

[a] Fragment sizes are given in kilobase pairs ± standard deviations based on the numbers of replicates (given in parentheses).
[b] Chromosome-specific genes or insertions hybridized to each fragment as indicated. SR, assigned on the basis of digestion of separated replicons.

(29). The primers 16S-11 and 16S-1507 amplified the region between bases 11 and 1507 in the 16S rRNA genes. The primers 23S2790R and 5S27L2 amplified the regions between bases 2790 and 27 in the 23S rRNA and in the adjacent 5S rRNA genes, respectively, and the spacer between them; this fragment is about 600 bp in length. PCR products were resolved by agarose gel electrophoresis, excised, and radiolabelled as probes in Southern hybridizations.

RESULTS

Genome size. Three restriction enzymes, *Pac*I (5′-TTAAT TAA-3′), *Swa*I (5′-ATTTAAAT-3′), and *Spe*I (5′-ACTAGT-3′), each of which cut the *R. meliloti* genome into fewer than 35 fragments, were previously identified (35, 36). We identified a fourth, rare-cutting restriction enzyme, *Pme*I (5′-GTTTA AAC-3′), which cut the entire *R. meliloti* 1021 genome into seven fragments. Both *Pac*I and *Swa*I linearize pSym-a (36), whereas *Pme*I cut this replicon into three fragments (see Table 4). The size estimate of pSym-b based on *Pme*I digestion (1,693 ± 100 kb) was consistent with estimates generated with *Pac*I and *Swa*I digests resolved by TAFE (36). The sum of *Spe*I fragments resolved by field inversion gel electrophoresis gave a slightly lower total size for pSym-b (36); however, when we resolved these fragments by TAFE, the resulting size estimate of pSym-b based on *Spe*I digestion was consistent with those generated by the other rare-cutting enzymes (see Table 3), suggesting that the estimation differences were due to differences in field geometries. The mean of all pSym-b size estimates was 1,720 ± 120 kb. The endonuclease I-*Ceu*I cuts within the 23S rRNA gene (10, 23, 24). *Pme*I and I-*Ceu*I each cut the chromosome into three fragments which gave sums of 3,560 and 3,610 kb, respectively (Table 2). These data are consistent with previous size estimates of 3,550 and 3,320 kb, based on *Swa*I and *Pac*I, respectively (36).

Construction of the chromosome map. The locations of genes and insertions from the chromosome are indicated in Table 2 and Fig. 1C. Both *gap1* and *glt* were located to Pme no. 4 by Southern hybridization. Hybridization (data not shown) of *Pme*I-*Swa*I double digests further localized *gap1* to a 170-kb *Pme*I-*Swa*I fragment and *glt* to a 495-kb *Pme*I-*Swa*I fragment, which confirmed the placement of a *Swa*I site within Pme no. 4. Further, hybridization to strain Rm7558 (containing an insertion in *lpsB*), as well as strain Rm8612 (containing the insertion Ω614), confirmed the placement of these genetic markers onto a 585-kb *Pme*I-*Swa*I fragment (data not shown). In addition, *ndvA* hybridized to a 100-kb *Pme*I-*Swa*I fragment (data not shown).

It was clear from gels that resolved the 620-kb *Swa*I doublet (upper fragment of 620 kb and lower fragment of 595 kb [sizes estimated from a single gel]) that the lower fragment contained the *Pac*I site. Placement of the *Pac*I site within this *Swa*I fragment was confirmed by digestion of strains A1681 (*ntrA*::Tn*5*) and Rm7558 (*lpsB*::Tn*5-104-3*), both of which are located on Pme no. 1 (Table 2). Hybridization to *Pac*I-*Pme*I digests of these strains resolved for fragments of 900 kb and less showed that *ntrA* was located on an 895-kb fragment and that *lpsB* was located on a fragment migrating in the compression zone (that is, greater than 900 kb), presumably the 1,020-kb *Pac*I-*Pme*I fragment (Table 2 and data not shown).

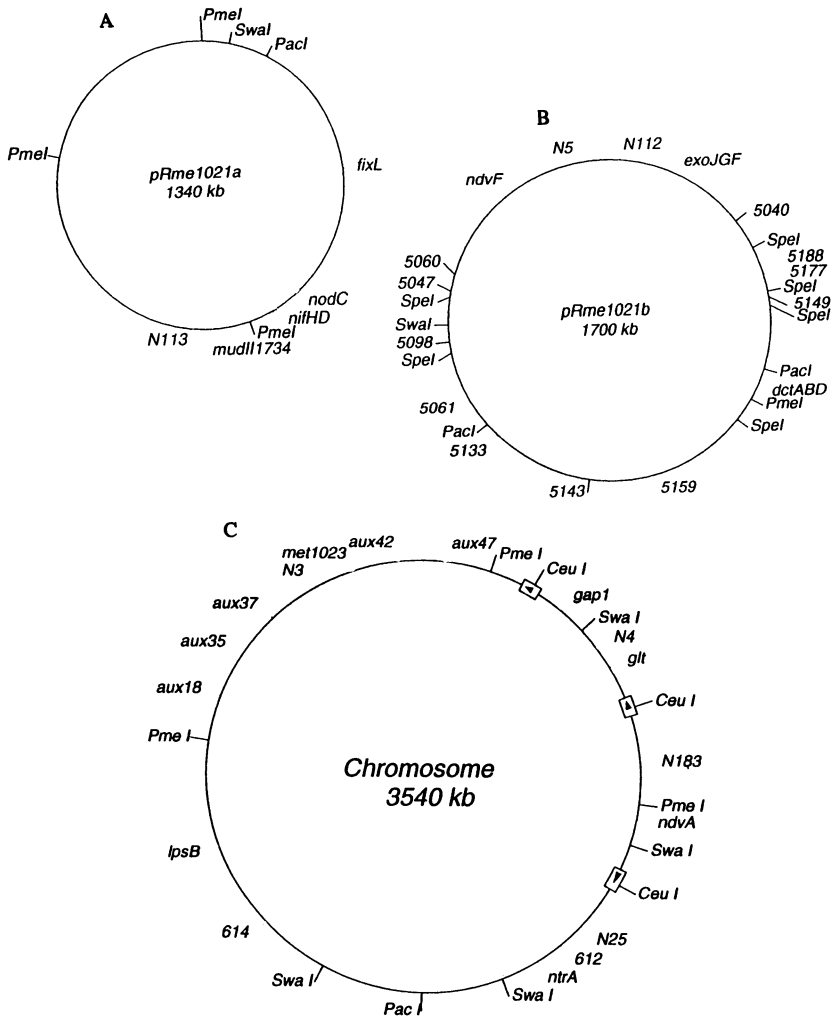

FIG. 1. Physical maps of the replicons of *R. meliloti* 1021. (A) pSym-a (1° ≈ 3.7 kb); (B) pSym-b (1° ≈ 4.7 kb); (C) chromosome (1° ≈ 9.8 kb). Arrows indicate the orientations of the *rrn* loci. For all replicons, solid lines indicate the positions of target sites and/or transposon insertions anchored to the physical map; the positional order shown for other markers residing on the same restriction fragment is random.

Placement and orientation of the *rrn* loci. Placement of an I-*Ceu*I site within Swa no. 6 was confirmed by hybridization of excised, radiolabelled Swa no. 6 to I-*Ceu*I–*Swa*I digests and by hybridization of *ndvA* to I-*Ceu*I–*Pme*I digests (Table 2). Hybridization of *ndvA* to *I-Ceu*I *Swa*I digests showed a I-*Ceu*I site within the 495-kb *Swa*I-*Pme*I fragment of Pme no. 4. Furthermore, *ntrA* hybridized to 615-kb I-*Ceu*I–*Pac*I fragment, which was consistent with the position of a *Pac*I site within the largest I-*Ceu*I fragment. When used as a probe, Ceu no. 3 hybridized to a 170-kb I-*Ceu*I–*Pme*I fragment in strain Rm5418 (*gap1*::Tn*5*). These data placed at least one I-*Ceu*I site adjacent to a *Pme*I site.

In *Escherichia coli*, the *rrn* loci are organized as follows: promoter$_1$-promoter$_2$-16S rRNA-tRNA-23S-rRNA-5S-rRNA-tRNA-terminator$_1$-terminator$_2$ (31). Primers that were designed to amplify a 1.5-kb internal region of the 16S *rrn* gene or a 0.6-kb region spanning part of the 23S rRNA gene and adjacent 5S rRNA gene (Fig. 2) were used in a standard PCR of genomic *R. meliloti* 1021 DNA. Because I-*Ceu*I cuts in the 23S rRNA, we hybridized the two probes to double digests of the rare-cutting enzymes to determine the orientation of the *rrn* loci. The amplified fragment was excised, radiolabelled, and used to probe *Spe*I, *Pac*I, *Swa*I, and *Pme*I digests. The labelled 16S rRNA and 23S-5S rDNA probes hybridized only to fragments previously assigned to the chromosome (Table 2). In addition, the 16S *rrn* probe hybridized to three *Spe*I fragments (about 300, 175, and 125 kb) assigned to the chromosome (15). The 16S probe also hybridized to three *Bam*HI and three *Hin*dIII fragments of total genomic digests. Control digests of the amplified fragment from *R. meliloti* showed that these enzymes do not cut within the region; these enzymes also do not cut within the corresponding region in *E. coli* or *Rhodobacter sphaeroides* sequences available in GenBank. Furthermore, in the example in Fig. 2, the 16S rRNA probe hybridized to Ceu no. 2 whereas the 23S-5S probe did not. Thus, the *rrn* loci in this fragment were divergent with only the 16S genes on the 520-kb fragment and the 23S genes on adjacent fragments in the map. The orientation of all *rrn* loci was determined by this strategy.

Construction of the pSym-b map. Fragments assigned to pSym-b are listed in Table 3. The *exoJGF* and *dctABC* genes hybridized to Pac no. 3 and no. 4, respectively, which suggested that one of the *Pac*I sites was located between 25° and 115° on the map. Furthermore, by hybridization of *ndvF* to Pac no. 3,

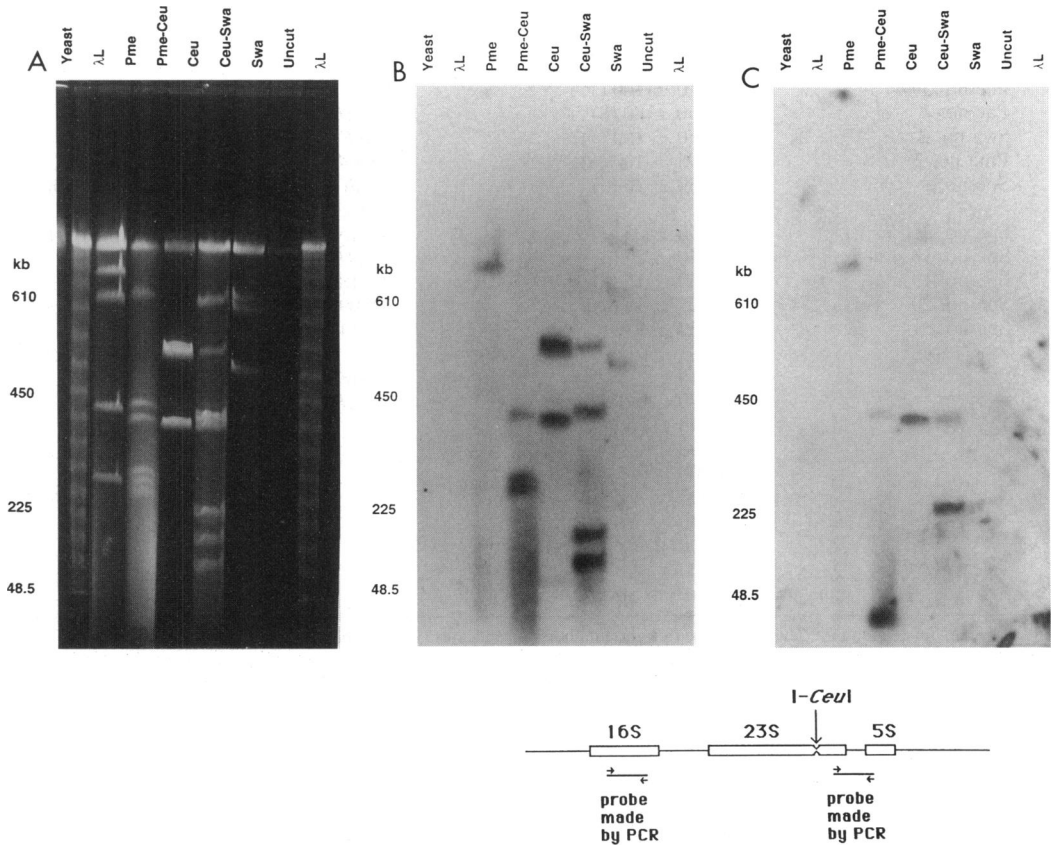

FIG. 2. Orientation of *rrn* loci on the chromosome of *R. meliloti* 1021. (A) TAFE gel (1% low EEO agarose in 0.25× Tris-borate-EDTA) of single and double digests of *R. meliloti* 1021 run at a 45-s pulse time with 350 mA of constant current for 36 h. Yeast chromosomes (Yeast) and lambda concatemers (λL) were used as size standards; sizes are indicated on the left of the gels in kilobases. Other lanes are as labelled. (B) Southern hybridization to blot of the TAFE gel shown in panel A, with the 16S probe indicated in the diagram below. (C) Southern hybridization to blot of TAFE gel shown in panel A, with the 23S-5S probe indicated in the diagram below.

the other *Pac*I site was confined to between 115° and 325° (clockwise) on the map. *Pac*I digests of selected Tn*5*-containing strains and hybridization with IS*50* confirmed the position of the second of the two *Pac*I sites. Ω5061::Tn*5-235* was located on Pac no. 3, whereas Ω5143::Tn*5-233* mapped to Pac no. 4. These data allowed us to position the second *Pac*I site to between 240° and 190°. The locations of the two *Pac*I sites are indicated in Fig. 1B.

The *ndvF* gene hybridized to Swa no. 2 (Table 3). To determine the position of the single *Swa*I site, the two *Pac*I fragments known to constitute pSymb were excised from a gel and then digested with *Swa*I and analyzed by TAFE. *Swa*I digestion of Pac no. 3 resulted in two fragments of about 1,000 and 200 kb, whereas Pac no. 4 was not cut by *Swa*I. These data indicated that the *Swa*I site was located about 40° (200 kb) from one end of Pac no. 3. A hybridizing fragment of 1,000 kb was found in a *Pac*I-*Swa*I double digest of RmF675 (Ω5188:Tn*5-132*). Therefore, the *Swa*I site is not located near 74° and must be near 270°. The placement of the *Swa*I site relative to the Ω5188 insertion at 264° was not determined.

*Pac*I-*Pme*I double digests of pSym-b gave three fragments: a 1,200-kb fragment (Pac no. 3), a 480-kb fragment, and a 70-kb fragment. The *dctABD* gene hybridized to the 70-kb fragment, which not only confirmed the position of the *Pme*I site within Pac no. 4 but also indicated that the site was within 15° (70 kb) of 115° (Fig. 1B).

Both *exoJGF* and *ndvF* hybridized to Spe no. 2, and *dctABD* hybridized to Spe no. 10 (Table 3 and data not shown). Furthermore, hybridization with *exoJGF* showed that Spe no. 2 was located within Pac no. 3. These data are consistent with the localization of one *Pac*I site between 25° and 115° on the map (Fig. 1B). *Pac*I-*Spe*I double digests revealed that Spe no. 10 contained a *Pac*I site (data not shown) and that Spe no. 3 also contained a *Pac*I site which resulted in two *Spe*I-*Pac*I fragments (approximately 410 and 120 kb) (data not shown). In strains F570 (Ω5159::Tn*5*), F470 (Ω5133::Tn*5*), and F221 (Ω5061::Tn*5-235*), the single hybridization fragment corresponded to Spe no. 3; therefore, this fragment must span 165°, 225°, and 240°. The position of Spe no. 19 was determined by hybridization of *Spe*I digests of strains containing Tn*5* or a derivative. Single hybridization fragments of 105 and 120 kb were observed for strains F675 and F601, respectively, which corresponded closely to the size of Spe no. 19 and indicated that this fragment spans 75° (Ω5188::Tn*5-132*) and 80° (Ω5177::Tn*5*).

Anchoring of the physical map to the genetic map of pSym-b by using Tn*5-233*. Hybridization of IS*50* to *Spe*I digests of genomic DNAs from strains 5404, F560, F532, F303, 5435, and F220 yielded two fragments each (Table 3 and data not shown). These strains contain the Tn*5* derivative Tn*5-233*, which has a unique 5.3-kb fragment from plasmid pSa (9). The presence of two hybridizing fragments in strains containing Tn*5-233* could be accounted for by the presence of a *Spe*I site

TABLE 3. Restriction fragments assigned to pRme1021b

Enzyme	Designation	Fragment size (kb)[a]	Identifying probe[b]
*Pac*I	Pac no. 3	1,210 ± 100 (17)	*exoJGF*, *ndvF*
	Pac no. 4	550 ± 80 (8)	*dctABD*
*Swa*I	Swa no. 2	1,650 ± 100 (7)	*ndvF*
*Pme*I	Pme no. 2	1,695 ± 100 (6)	Ω*5040*
*Spe*I	Spe no. 2	650 ± 20 (3)	*exoJGF*, *ndvF*, N5, N112, Ω5040 (590 + 50)[c], Ω5047 (625 + 20), Ω5060 (600 + 75)
	Spe no. 3	590 ± 25 (3)	Ω5159, Ω5133, Ω5061, Ω5143 (505 + 105)
	Spe no. 10	240 ± 20 (4)	*dctABD*, N12, N110
	Spe no. 19	130 ± 15 (4)	Ω5188, Ω5177
	Spe no. 20	125 ± 15 (4)	Ω5098 (100 + 20)
	Spe no. 31	33 ± 9 (3)	Ω5149 (15 + 5)
*Pac*I + *Swa*I		195	
		1,110	Ω5188
*Pac*I + *Pme*I		70	*dctABD*
		490	
*Swa*I + *Pme*I		690	
		1,000	
*Pac*I + *Spe*I		95	
		140	
*Pme*I + *Spe*I		30	
		200	
*Swa*I + *Spe*I		cuts small piece from Spe #3 or Spe #20	

[a] Sizes are given in kilobase pairs ± standard deviations based on the numbers of replicates (given in parentheses) by TAFE.
[b] pSym-b-specific genes or insertions hybridized to each fragment as indicated.
[c] The sizes of the hybridizing fragments for insertions of Tn*5-233* are given in kilobases. Note that the sum of the two fragments is in agreement with the size of the respective *Spe*I fragment.

within the unique 5.3-kb fragment. The presence of a *Spe*I site within the insertion allowed us to use these inserts as linking probes to anchor the physical map to the genetic map. In this way, the distance from a known insertion to the nearest *Spe*I site could be determined. For example, in strain 5404, two hybridization fragments of 590 and 50 kb were observed (data not shown). The sum of the two hybridization fragments corresponded to the size of Spe no. 2 (Table 3). These data indicated that Spe no. 2 ends approximately 10° clockwise (that is, at 65°) to the insertion site of Ω5040::Tn*5-233* at 53° on the map and are consistent with the positioning of Spe no. 2 to span the *exoJGF* locus at 25°. The two hybridizing fragments in strain F560 give a sum of 20 kb (data not shown), indicating that Spe no. 31 spans the 80° position of Ω5149::Tn*5-233*. The remaining *Spe*I fragment, Spe no. 20, is located between Spe no. 2 and no. 3 as defined by the insertion at 264° of Ω5098::Tn*5-233*, as shown in Fig. 1B.

Construction of the pSym-a map. The physical locations of genetic markers from pSym-a are shown in Table 4. The relative order of these genetic markers was determined previously; specifically, *fixL* is located about 220 kb to one side of the *nod-nif* cluster (7), and mu*dII1734* is about 40 kb to the other side of the *nod-nif* cluster (30). Because mu*dII1734* is located on Pme no. 6 and both *nodC* and *nifHD* are located on Pme no. 5, a *Pme*I site must be located near 180° on the physical map (Fig. 1A). *Pac*I-*Pme*I and *Pac*I-*Swa*I digests of separated replicon pSym-a each yielded one large fragment and one small fragment (<100 kb) (Table 4). Hybridization data (not shown) of *Pac*I-*Swa*I, *Pac*I-*Pme*I, and *Pme*I-*Swa*I digests with *nifHD* showed that the *nod-nif* cluster is located on a 1,265-, 520-, and 600-kb fragment, respectively (Table 4). These data confirmed the positions of the *Pac*I and *Swa*I sites, the relative order of the *Pme*I fragments, and the orientation of Pme no. 5 and no. 6.

TABLE 4. Restriction fragments assigned to pRme1021a

Enzyme	Designation	Fragment size (kb)[a]	Identifying probe[b]
*Pac*I	Pac no. 2	1,420 ± 130 (16)	*nodC*, *nifHD*
*Pme*I	Pme no. 5	600 ± 60 (8)	*nifHD*, *fixL*
	Pme no. 6	420 ± 35 (8)	mu*dII1734*, N113
	Pme no. 7	305 ± 30 (8)	SR
*Swa*I	Swa no. 3	1,340 ± 90 (7)	*nifHD*
*Pac*I + *Swa*I		60	SR
		1,265	*nifHD*
*Pac*I + *Pme*I		100	SR
		520	*nifHD*
*Pme*I + *Swa*I		35	SR
		600	*nifHD*

[a] Fragment sizes are given in kilobase pairs ± standard deviations based on the numbers of replicates (given in parentheses).
[b] pSym-a-specific genes hybridized to each fragment as indicated. SR, assignment based on digestion of separated replicons.

Use of the physical map to quickly localize novel insertions. *R. meliloti* strains containing Tn*5* inserted at unknown locations in the genome were used to rapidly add new markers to the maps. The phenotypes exhibited by these strains are described elsewhere (22). The locations of the insertions were determined by *Pme*I digestion and then by Southern hybridization. This allowed us to immediately determine which replicon contained the insertion; in the case of pSym-a and the chromosome, this single experiment also located the insertion with respect to known restriction sites. As an example, the insertion in strain N4 was located on Pme no. 4, so to refine its position within the fragment a second experiment was done with informative enzymes for double digests (*Swa*I or I-*Ceu*I in this example). Of 35 strains containing Tn*5*, 3 gave restriction patterns with two separate single enzyme digests that were different from that of the mapped strain, which indicated that a rearrangement had occurred. These 3 strains were not studied further. Insertions from 12 of the remaining 32 strains are mapped in Fig. 1, and 9 additional insertions are located to single-digest products (Tables 2 and 3); however, their locations have not been further refined.

DISCUSSION

Genome size and the chromosome map. We have generated the first complete physical map of the genome of *R. meliloti* (Fig. 1). The estimated sizes of the three replicons agree closely with prior PFGE estimates (35, 36), with electron microscopy measurements (2, 3), and, in the case of pSym-b, with the genetic map (5, 6). The relative order of genetic markers located on the *R. meliloti* chromosome map described by Glazebrook et al. (13) is also consistent with their respective physical-map locations. The physical-map location of *gap1* is consistent with its genetic-map location between *leu53* and *trp33* auxotrophic markers (12). Such previously mapped markers on the genetic map aided in the ordering of restriction fragments and, in some instances, permitted anchoring of the genetic markers to specific points on the physical map, as described below for pSym-b. The *glt* locus (21) was not located on the chromosomal genetic map; however, because we have located *glt* on the physical map, its relative genetic-map location is now known. Similarly, newly identified genes can be readily positioned on the maps.

Placement and orientation of *rrn* loci and use of I-*Ceu*I. The use of I-*Ceu*I in PFGE physical mapping (23) allows the determination of the numbers and locations of *rrn* loci in the physical maps of eubacteria. This is because the enzyme cleaves only at a relatively long sequence of greater than 10 bp that occurs in a region of the 23S rRNA gene that is highly conserved among eubacteria. We found that three *rrn* loci exist in the *R. meliloti* genome and that these are all located on the largest of the three replicons. Three *rrn* loci are also found in *R. sphaeroides*, although in *R. sphaeroides* these three loci are distributed onto two replicons (one *rrn* locus on the 3,046-kb replicon and two *rrn* loci on the 914-kb replicon) (38). Using probes within the *rrn* gene that flank the I-*Ceu*I site, we were able to determine the orientation of these loci in the *R. meliloti* chromosome. Interestingly, the *rrn* loci are clustered in one region of the chromosome, as they are in *Salmonella typhimurium* and *E. coli*. Furthermore, it has been noted previously that the orientation of *rrn* is away from the origin of replication in *E. coli* (1) and *S. typhimurium* (32). The orientation of *rrn* in *R. meliloti* is also such that if the origin is in the 520-kb I-*Ceu*I fragment, then of all the *rrn* loci would point away from the origin. Thus, it is possible that the orientations are selected for and that orientation of *rrn* transcription away from the origin may be a general rule for at least some gram-negative bacteria.

There is a small possibility that I-*Ceu*I does not cut all *rrn* loci. It is also possible that I-*Ceu*I occasionally cleaves at sites other than *rrn* loci. The presence of a partial I-*Ceu*I digest product of 425 kb and the hybridization of Ceu no. 3 to this fragment indicated that a 30-kb fragment may contain a 4th *rrn* locus adjacent to Ceu no. 3, although neither the 16S nor the 23S-5S *rrn* probe hybridizes to this small fragment. In the physical map of *R. meliloti* 1021, there are few places where such an *rrn* cluster could reside without being detected as an anomaly in the Southern blots by using *rrn* probes. Also, all I-*Ceu*I cleavage sites are associated with *rrn*, as demonstrated by Southern blots. In *S. typhimurium*, all six *rrn* loci are cleaved (23) and no sites other than *rrn* loci are cleaved. We sometimes detected faint, persistent partial cleavage products for I-*Ceu*I which, when taken into account, actually helped to determine adjacent fragments on the physical map.

The pSym-b map. The physical maps of pSym-b and the chromosome are closely correlated with the previously established genetic maps of these replicons (5, 6, 13). The physical distances calculated from transduction frequencies of genetic markers on pSym-b (6) correlate with size estimates based on summing of restriction fragments, and the relative order of genetic markers was found to be consistent with physical map locations (Fig. 1B). Six genetic markers, defined by an insertion of the Tn*5-233* derivative, permitted us to anchor the physical map of pSym-b to its genetic map. Tn*5-233* could be used to replace other Tn*5* derivatives inserted in the genome and to allow the locus to be mapped in relation to other *Spe*I sites.

Wong and McClelland (40, 41) have described the construction of a mini-Tn*5* containing rare restriction endonuclease target sites. The mini-Tn*5* construct does not transpose efficiently in *Rhizobium* species (39a). We are currently modifying existing Tn*5* derivatives that transpose in *Rhizobium* species (such as Tn*5-233*) to carry rare restriction sites.

The pSym-a map. We found that the physical map of pSym-a correlates well with the genetically mapped regions. At least 15 genes in the *nod-nif* cluster of *R. meliloti* have been cloned (37); however, the remainder of this replicon lacks genetic markers. The lack of either cloned genes or transposon insertions precludes a more detailed map at present. *Spe*I cuts pSym-a into at least 12 fragments (15), although the sites are distributed unevenly throughout the replicon. Only one fragment is greater than 350 kb, with the remainder being 125 kb and less. Similar asymmetry of sites is observed with *Ase*I (15). These observations suggest that the nucleotide composition may differ in the genome. Burkhardt et al. (3) reported the GC content for pSym-a to be 57.5 to 58.6% and reported higher GC contents for pSym-b and the chromosome (61.7%). Dylan (11) analyzed the base composition at each codon position in the sequences of symbiotic and asymbiotic genes from *Rhizobium* species, *Bradyrhizobium* species, and *Klebsiella pneumoniae*. He concluded that the symbiotic genes from *Rhizobium* and *Bradyrhizobium* species must have been acquired from a source with a more-AT-rich third-position profile. The base usage in the third position in *nod*, *nif*, and *fix* genes is distinct from those in asymbiotic genes located on the chromosome in *Rhizobium* species, suggesting that at least part of the genome may have a different evolutionary history.

Applying the map: an example of rapid localization of Tn*5* insertions. The physical map of *R. meliloti* should be a valuable resource for rapidly assigning markers to a region within a particular replicon. Furthermore, if a gene is tagged with a transposon carrying a cleavage site that is rare in the genome (such as Tn*5-233* carrying *Spe*I integrated into pSym-b), then the insertion can be mapped to within a few kilobases. In addition, the physical map of any new transposon-containing strain can be used to determine whether rearrangements that would remain unrecognized in genetic mapping have occurred. Furthermore, the physical maps of other strains of *R. meliloti* or related species can now be quickly generated to allow comparisons of evolutionarily conserved regions of the genomes.

ACKNOWLEDGMENTS

We thank the persons cited in Table 1 for their gifts of bacterial strains and clones used in this study. We also thank Graham Walker, Massachusetts Institute of Technology, and Frans de Bruijn, Michigan State University, for sharing data prior to publication and Dave Ralph, CIBR, for providing the *rrn* primers and for critical reading of the manuscript.

This work was supported by grant no. 9103456 from the U.S. Department of Agriculture to B.W.S.S. M.M. was supported in part by NIH grant 2R01AI34829.

REFERENCES

1. **Brewer, B.** 1988. When polymerases collide: replication and the transcriptional organization of the *E. coli* chromosome. Cell **53**:679–686.

2. **Burkhardt, B., and H. J. Burkhardt.** 1984. Visualization and exact molecular weight determination of a *Rhizobium meliloti* megaplasmid. J. Mol. Biol. **175:**213–218.
3. **Burkhardt, B., D. Schillik, and A. Puhler.** 1987. Physical characterization of *Rhizobium meliloti* megaplasmids. Plasmid **17:**13–25.
4. **Casadeus, J., and J. Olivares.** 1979. Rough and fine linkage mapping of the *Rhizobium meliloti* chromosome. Mol. Gen. Genet. **174:**203–209.
5. **Charles, T. C., and T. M. Finan.** 1990. Genetic map of *Rhizobium meliloti* megaplasmid pRmeSU47b. J. Bacteriol. **172:**2469–2476.
6. **Charles, T. C., and T. M. Finan.** 1991. Analysis of a 1600-kilobase *Rhizobium meliloti* megaplasmid using defined deletions generated *in vitro*. Genetics **127:**5–20.
7. **David, M., M.-L. Daveran, J. Batut, A. Dedieu, O. Domergue, J. Ghai, C. Hertig, P. Boistard, and D. Kahn.** 1988. Cascade regulation of *nif* gene expression in *Rhizobium meliloti*. Cell **54:**671–683.
8. **Denarie, J., P. Boistard, F. Casse-Delbart, A. G. Atherly, J. O. Berry, and P. Russell.** 1981. Indigenous plasmids of *Rhizobium*, p. 225–246. *In* K. L. Giles and A. G. Atherly (ed.), Biology of the *Rhizobiaceae*. Academic Press, New York.
9. **DeVos, G. F., G. C. Walker, and E. R. Signer.** 1986. Genetic manipulations in *Rhizobium meliloti* utilizing two new transposon Tn5 derivatives. Mol. Gen. Genet. **204:**485–491.
10. **Dujon, B., M. Belfort, R. A. Butow, C. Jacq, C. Lemieux, P. S. Perlman, and V. M. Vogt.** 1989. Mobile introns: definition of terms and recommended nomenclature. Gene **82:**115–118.
11. **Dylan, T. M.** 1989. Ph.D. dissertation. University of California at San Diego, La Jolla.
12. **Finan, T. M., I. Oresnik, and A. Bottacin.** 1988. Mutants of *Rhizobium meliloti* defective in succinate metabolism. J. Bacteriol. **170:**3396–3403.
13. **Glazebrook, J., G. Meiri, and G. Walker.** 1992. Genetic mapping of symbiotic loci on the *Rhizobium meliloti* chromosome. Mol. Plant-Microbe Interact. **5:**223–227.
14. **Hennecke, H., K. Kaluza, B. Thony, M. Fuhrmann, W. Ludwig, and E. Stackebrandt.** 1985. Concurrent evolution of nitrogenase genes and 16S rRNA in *Rhizobium* species and other nitrogen fixing bacteria. Arch. Microbiol. **142:**342–348.
15. **Honeycutt, R. J.** 1991. Ph.D. dissertation. Iowa State University, Ames.
16. **Huguet, T., C. Rosenberg, F. Casse-Delbart, P. de Lajudie, L. Jouanin, J. Batut, P. Boistard, J. S. Julliot, and J. Denarie.** 1983. Studies on *Rhizobium meliloti* plasmids and their role in the control of nodule formation and nitrogen fixation: the pSym megaplasmids and other large plasmids, p. 35–45. *In* A. Puhler (ed.), Molecular genetics of the bacteria-plant interaction. Springer-Verlag, Berlin.
17. **Jordan, D. C.** 1984. Rhizobiaceae, p. 234–244. *In* N. R. Krieg, and J. G. Holt (ed.), Bergey's manual of systematic bacteriology, vol. 1. Williams & Wilkins, Baltimore.
18. **Kohara, Y.** 1990. Correlation between the physical and genetic maps of the *Escherichia coli* K-12 chromosome, p. 29–42. *In* K. Drlica and M. Riley (ed.), The bacterial chromosome. American Society for Microbiology, Washington, D.C.
19. **Krawiec, S., and M. Riley.** 1991. Organization of the bacterial chromosome. Microbiol. Rev. **54:**502–539.
20. **Kundig, C., H. Hennecke, and M. Gottfert.** 1993. Correlated physical and genetic map of the *Bradyrhizobium japonicum* 110 genome. J. Bacteriol. **175:**613–622.
21. **Lewis, T. A., R. Gonzalez, and J. L. Botsford.** 1990. *Rhizobium meliloti* glutamate synthase: cloning and initial characterization of the *glt* locus. J. Bacteriol. **172:**2413–2420.
22. **Lim, P. O., D. Ragatz, L. Kragelund, P. Wolk, M. Renner, and F. J. de Bruijn.** Unpublished data.
23. **Liu, S.-H., A. Hessel, and K. E. Sanderson.** Genomic mapping with I-*Ceu*I, an intron-encoded endonuclease specific for genes for ribosomal RNA in *Salmonella* spp., *E. coli*, and other bacteria. Proc. Natl. Acad. Sci. USA **90:**6874–6878.
24. **Marshall, P., and C. Lemieux.** 1992. The I-*Ceu*I endonuclease recognizes a sequence of 19 base pairs and preferentially cleaves the coding strand of the *Chlamydomonas moewusii* chloroplast large subunit rRNA gene. Nucleic Acids Res. **20:**6401–6407.
25. **Martinez, E., D. Romero, and R. Palacios.** 1990. The *Rhizobium* genome. Crit. Rev. Plant Sci. **9:**59–93.
26. **McClelland, M., R. Jones, Y. Patel, and M. Nelson.** 1987. Restriction endonucleases for pulsed field mapping of bacterial genomes. Nucleic Acids Res. **15:**5985–6005.
27. **Meade, H. M., and E. R. Signer.** 1977. Genetic mapping of *Rhizobium meliloti*. Proc. Natl. Acad. Sci. USA **74:**2076–2078.
28. **Perret, X., W. J. Broughton, and S. Brenner.** 1991. Canonical ordered cosmid library of the symbiotic plasmid of *Rhizobium* species NGR234. Proc. Natl. Acad. Sci. USA **88:**1923–1927.
29. **Ralph, D., M. McClelland, J. Welsh, G. Baranton, and P. Perolat.** 1993. *Leptospira* species categorized by arbitrarily primed polymerase chain reaction (PCR) and by mapped restriction polymorphisms in PCR-amplified rDNA genes. J. Bacteriol. **175:**973–981.
30. **Renalier, M.-H., J. Batut, J. Ghai, B. Terzaghi, M. Gherardi, M. David, A.-M. Garnerone, J. Vasse, G. Truchet, T. Huguet, and P. Boistard.** 1987. A new symbiotic cluster on the pSym megaplasmid of *Rhizobium meliloti* 2011 carries a functional *fix* gene repeat and a *nod* locus. J. Bacteriol. **169:**2231–2238.
31. **Riley, M., and S. Krawiec.** 1987. Genome organization, p. 967–981. *In* F. C. Neidhardt, J. L. Ingraham, K. B. Low, B. Magasanik, M. Schaechter, and H. E. Umbarger (ed.), *Escherichia coli* and *Salmonella typhimurium*: cellular and molecular biology. American Society for Microbiology, Washington, D.C.
32. **Riley, M., and K. Sanderson.** 1990. Comparative genetics of *E. coli* and *S. typhimurium*, p. 85–95. *In* K. Drlica, and M. Riley (ed.), The bacterial chromosome. American Society for Microbiology, Washington, D.C.
33. **Sambrook, J., E. F. Fritsch, and T. Maniatis.** 1989. Molecular cloning: a laboratory manual. Cold Spring Harbor Laboratory, Cold Spring Harbor, N.Y.
34. **Schwartz, D. C., and C. R. Cantor.** 1984. Separation of chromosome-sized DNAs by pulsed-field gradient gel electrophoresis. Cell **37:**67–75.
35. **Sobral, B. W. S., R. J. Honeycutt, and A. G. Atherly.** 1991. The genomes of the family *Rhizobiaceae*: size, stability, and rarely cutting restriction endonucleases. J. Bacteriol. **173:**704–709.
36. **Sobral, B. W. S., R. J. Honeycutt, A. G. Atherly, and M. McClelland.** 1991. Electrophoretic separation of the three *Rhizobium meliloti* replicons. J. Bacteriol. **173:**5173–5180.
37. **Sobral, B. W. S., R. J. Honeycutt, A. G. Atherly, and K. D. Noel.** 1991. Recognition and infection in legume nodulation, p. 229–258. *In* M. J. Dilworth and A. R. Glenn (ed.), Biology and biochemistry of nitrogen fixation. Elsevier, Amsterdam.
38. **Suwanto, A., and S. Kaplan.** 1989. Physical and genetic mapping of the *Rhodobacter sphaeroides* 2.4.1 genome: presence of two unique circular chromosomes. J. Bacteriol. **171:**5850–5859.
39. **Weisburg, W. G., S. M. Burns, D. A. Pelletier, and D. Lane.** 1991. 16S ribosomal DNA amplification for phylogenetic study. J. Bacteriol. **173:**697–703.

39a. **Wong, K. K.** Personal communication.

40. **Wong, K. K., and M. McClelland.** 1992. Dissection of the *Salmonella typhimurium* genome by use of a Tn5 derivative carrying rare restriction sites. J. Bacteriol. **174:**3807–3811.
41. **Wong, K. K., and M. McClelland.** 1992. A Bln restriction map of the *Salmonella typhimurium* genome. J. Bacteriol. **174:**1656–1661.